Separation Science and Technology
Publication details, including instructions for authors and subscription information:
http://www.informaworld.com/smpp/title~content=t713708471

STEADY STATE SIMULATION OF PHOSPHORIC ACID CONCENTRATION PROCESS

Oumkeltoum Bennouna[a]; Tijani Bounahmidi[a]
[a] Département Génie des Procédés, Ecole Mohammadia d'Ingénieurs, Rabat, Morocco

Online publication date: 08 May 2002

To cite this Article Bennouna, Oumkeltoum and Bounahmidi, Tijani(2002) 'STEADY STATE SIMULATION OF PHOSPHORIC ACID CONCENTRATION PROCESS', Separation Science and Technology, 37: 12, 2939 — 2966
To link to this Article: DOI: 10.1081/SS-120005474
URL: http://dx.doi.org/10.1081/SS-120005474

SEPARATION SCIENCE AND TECHNOLOGY, 37(12), 2939–2966 (2002)

STEADY STATE SIMULATION OF PHOSPHORIC ACID CONCENTRATION PROCESS

Oumkeltoum Bennouna and Tijani Bounahmidi*

LASPI, Département Génie des Procédés,
Ecole Mohammadia d'Ingénieurs, Avenue IBN SINA,
B.P. 765, Agdal, Rabat, Morocco

ABSTRACT

Steady-state simulation of wet phosphoric acid concentration process was carried out using process engineering simulator SCAPE (Software for Computer Aided Process Engineering), with the aim to study process performances. Industrial phosphoric acid was characterized by a mixture of phosphoric acid, water, and impurities in aqueous solution. The major phosphoric acid impurities were represented by a pseudocomponent. The Peng–Robinson equation of state was adapted to calculate phase equilibrium for industrial phosphoric acid using the pseudo-component approach. The simulation of many points of cycle of phosphoric acid concentration process was carried out. The results obtained were compared to process data. The mean absolute relative error was within 0.4% for boiler temperature, 0.9% for heat exchanger outlet temperature, 0.3% for P_2O_5 mass content of concentrated phosphoric acid, and 0.4% for concentrated phosphoric acid mass flow rate. The sensitivity of P_2O_5 mass

*Corresponding author. Fax: +212-37-687167; E-mail: tijani@emi.ac.ma

concentration of concentrated phosphoric acid vs. the main process parameters such as steam and weak phosphoric acid feeds, boiler pressure, and impurities mass content of weak phosphoric acid was studied.

Key Words: Industrial phosphoric acid; Pseudocomponent; Impurities; Concentration; Simulation; Process simulator

INTRODUCTION

Phosphoric acid, when produced from the dihydrate process, at about 28–30% P_2O_5, in most cases must be concentrated to about 54% P_2O_5 grade acid. The concentration process used frequently is based on evaporation under vacuum.

In this process, the weak phosphoric acid feed is mixed with strong acid bled off from the evaporator by a circulating pump (Fig. 1) through an impregnated graphite blocks heat exchanger.

The heat transfer rate from the low-pressure steam is used to carry the acids mixture to the boiling point temperature, corresponding to evaporator pressure of about 60 mmHg.

During concentration, scaling of the heat exchanger surfaces due to dissolved mineral salts, and the adverse physical properties of the acid made the process difficult to operate. This scaling has been of most concern because of breakage of the fragile impregnated graphite tubes and reduction of heat transfer rates resulting in increased maintenance cost, down production time and rates. Several studies provided comprehensive reviews of scaling problems.[1–4]

The computer aided process simulation is universally recognized as an essential tool in the chemical process industries.

The thermodynamic equilibrium for the phosphoric acid, and the physical properties of the latter are invariably the most important and the most difficult part of simulation.[5–13]

Not many works were published in the literature on the modeling and simulation of phosphoric acid production process. The hemihydrate and dihydrate process simulation has appeared in some references.[14–17] Other investigations concerning the wet phosphoric acid impurities were reported in the literature.[18–20]

The objective of the present work is the steady state simulation of phosphoric acid concentration process (Fig. 1). The simulation was performed

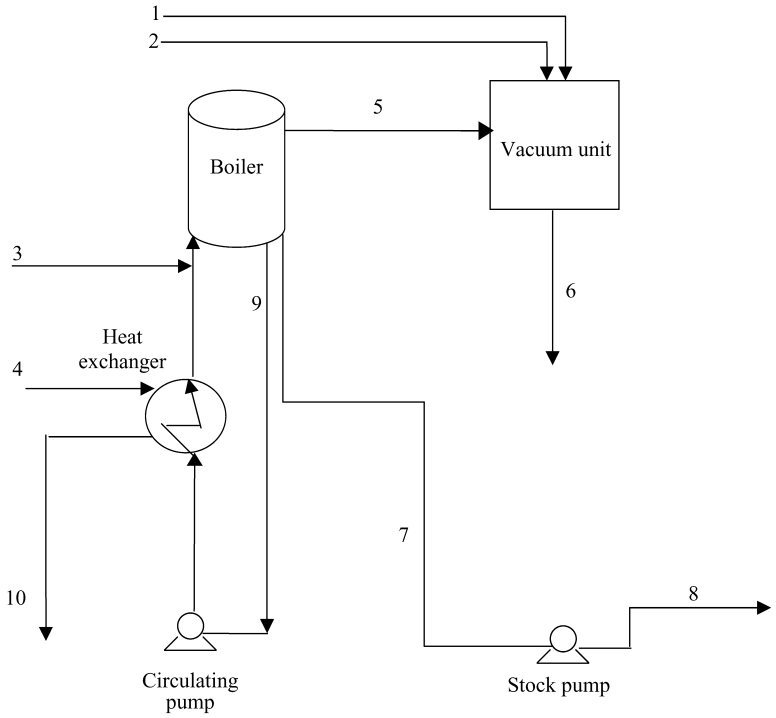

Figure 1. Phosphoric acid concentration process flow-sheet. 1: Pressure mean vapor feed. 2: Sea water. 3: Feed of phosphoric acid about 30% P_2O_5. 4: Feed of low pressure steam. 5: Vapor phase from boiler. 7: Concentrated phosphoric acid to about 54% P_2O_5. 8: Storage of product phosphoric acid. 9: Recycled phosphoric acid from boiler. 10: Condensed steam.

using equation of state and the pseudocomponent approach for modeling the vapor–liquid equilibrium (VLE) of industrial phosphoric acid. Software for Computer Aided Process Engineering (SCAPE) sequential modular process simulator developed previously in our laboratory was employed for this task.

ESTIMATION OF THERMODYNAMIC PROPERTIES

The industrial phosphoric acid of about 30% P_2O_5 contains several types of ions and compounds in solution in a saturated or supersaturated state. As the acid

is concentrated, the solubility of many of these compounds is exceeded, giving rise to the precipitation of several solids.[21,22]

For such complex systems, equation of state combined with pseudocomponent approach permit to describe more easily the VLE behavior. Indeed, this approach was used recently in our laboratory for good estimation of boiling temperature of industrial cane and beet sugar juices.[23]

In the present article, we apply the same approach for industrial phosphoric acid VLE estimation. In this respect, as for industrial sugar juices, the Peng–Robinson (PR) equation of state was used and all the ionic impurities of this acid were lumped in the same pseudocomponent. Thus the industrial phosphoric acid was considered as a ternary system: H_3PO_4–H_2O–impurities.The solid phase formed in the solution was also represented by the same pseudocomponent.

On the basis of the literature,[21,22] the pseudocomponent was assumed to be constituted by the following salts: [$Al(H_2PO_4)_3$, CaF_2, $Ca(H_2PO_4)_2$, $CaSiF_6$, $CaSO_4$, $Fe(H_2PO_4)_2$, K_2SiF_6, K_3AlF_6, $MgCl_2$, $MgSiF_6$, Na_2SiF_6, Na_3AlF_3].

The Peng–Robinson Equation of State[25]

This equation can be used to describe the behavior of the vapor phase as well as that of liquid phase.

For a pure substance, Peng–Robinson Equation of State (PR EOS) is given by the following expression:

$$P = \frac{RT}{v - b} - \frac{a(T)}{v^2 + 2bv - b^2} \tag{1}$$

where a and b are functions of critical temperature T_c, critical pressure P_c and acentric factor, ω; R is the universal gas constant; T is the temperature (K), and v is the molar volume.

For mixtures, the usual following mixing rules were used:

$$a_m = \sum_i \sum_j z_i z_j (1 - \delta_{ij})(a_i a_j)^{0.5} \tag{2}$$

$$b_m = \sum_i z_i b_i \tag{3}$$

where z_i is the fraction of component i and δ_{ij} the binary interaction parameter between components i and j.

The acentric factor was calculated using Edmister's relation:[26]

$$\omega = \frac{3}{7}\left(\frac{\mathrm{Log}_{10} P_c}{T_c/T_b - 1}\right) - 1 \tag{4}$$

where T_b is the boiling temperature.

Prediction of Phase Equilibrium

The conditions of VLE for a mixture of n components are:

$$f_i^V = f_i^L \quad (i = 1, \ldots, n) \tag{5}$$

where f_i^V and f_i^L are the fugacities of the component i in the vapor and liquid phases, respectively.

The fugacity f_i of a component i in a mixture, is related to its mole fraction z_i and to the total pressure P by Eq. (6).

$$f_i = \phi_i z_i P \tag{6}$$

The fugacity coefficient ϕ_i is calculated using PR EOS.[27]

Adaptation of PR EOS to Industrial Phosphoric Acid Solution

Estimation of Pseudocomponent Properties

In order to estimate the fossil-fuel EOS constants, Alexander et al.[24] established correlations relating these constants to characterization data using model fluids. Their regressions show that these EOS constants depend on molecule size, molecular shape, and charge distribution. These features can be well represented by the number of each type of hydrogen atoms and heteroatoms, per molecule. The same method was also used to evaluate PR EOS constants for industrial sugar juices.[23]

This principle was applied in the present work to estimate the pseudocomponent physical properties. Indeed, multiple stepwise regressions were developed to correlate critical temperature T_c, critical pressure P_c, and boiling point temperature T_b to the ionic structural characterization for 27 pure compounds model

given in Table 1, which are formed by ions constituting the salts considered in the pseudocomponent. The Eqs. (7)–(9) were obtained respectively:

$$\begin{aligned} T_c = {} & 2251.934 + 1544.324Al^{3+} + 2891.777(Ca^{2+})^{-1/2} \\ & - 881.409Cl^- - 286.431F^- + 1491.734Fe^{2+} + 959.110K^+ \\ & + 3698.066Mg^{2+} + 2029.475(Na^+)^{1/2} - 638.677OH^- \\ & - 1783.258(P^{5+})^{-1} - 51.400S^{2-} + 1851.575Si^{4+} \\ & - 174.344(Al^{3+})^{1/2}Cl^- - 716.431Cl^-Mg^{2+} \\ & + 917.211Cl^-P^{5+} + +56.686Cl^-S^{2-} - 822.732(Na^+)^{1/2}OH^- \\ & - 45.345O^{2-}P^{5+} \end{aligned} \tag{7}$$

$$\begin{aligned} P_c = {} & 58.180 + 947.510Al^{3+} + 318.730(Ca^{2+})^2 + 306.200Fe^{2+} \\ & + 183.133(K^+)^{1/2} - 24.270(Mg^{2+})^{-1} + 224.476Na^+ \\ & - 29.346OH^- + 49.984P^{5+} - 52.523(P^{5+})^{-1/2} \\ & + 278.000(Si^{4+})^2 - 326.447Al^{3+}Cl^- - 302.293Al^{3+}F^- \\ & + 136.620(Cl^-)^{1/2}Mg^{2+} - 94.950Cl^-Fe^{2+} \\ & + 72.344Cl^-(Na^+)^{1/2} - 1382.976(Cl^-)^{1/2}Si^{4+} \\ & + 663.914Cl^-(Si^{4+})^{1/2} - 7.485O^{2-}P^{5+} \\ & + 49.133(OH^-)^{1/2}(S^{2-})^{1/2} \end{aligned} \tag{8}$$

Table 1. T_c, P_c, and T_b for 27 Mineral Substances Model[26]

Substance	T_c (K)	P_c (bar)	T_b (K)
$AlCl_3$	629	26.35	453.15
AlF_3	2948.13	98.81	1810.15
Al_2O_3	5335	1953.20	3253.15
CaF_2	4570.85	376.91	2806.50
$FeCl_2$	2115.88	174.48	1299.15
$FeCl_3$	964.41	79.53	592.15
H_2SO_4	925	64	610
KF	2891.12	238.40	1775.15
KOH	2605.86	214.88	1600
$MgCl_2$	2754.32	227.12	1691.15
MgO	5950	33.91	3873.20
NaCl	3400	355	1738.15
NaOH	2820	253.31	1663.15
PCl_3	563.15	56.7	349.25
PCl_5	646.15	58.15	433
$POCl_3$	602.15	51.66	378.65
PSCl3	638.82	48.57	398.15
P_4O_6	714.86	52.08	446.25
P_4S_{10}	1291	232	787.15
$SOCl_2$	567	63.63	348.75
SO_2Cl_2	545	46.10	342.55
SO_3HCl	700	85	427
S_2Cl_2	659.37	62.75	411.15
SiO_2	4076.87	336.18	2503.2
Si_2Cl_6	660.96	29.11	412.15
Si_2OCl_6	655.58	27.90	408.75
Si_3Cl_8	775.41	24.70	484.55

$$\begin{aligned} T_b = {} & 1381.690 + 937.003Al^{3+} + 1767.234(Ca^{2+})^2 - 540.635Cl^- \\ & - 171.212F^- + 915.548Fe^{2+} + 579.950K^+ + 2491.510Mg^{2+} \\ & + 897.095(Na^+)^{1/2} - 376.918OH^- - 1135.928(P^{5+})^{-1} \\ & - 30.954S^{2-} + 1138.645Si^{4+} - 140.664Al^{3+}(Cl^-)^{1/2} \\ & - 778.369(Cl^-)^{1/2}Mg^{2+} + 578.305Cl^-(P^{5+})^{1/2} \\ & + 35.297Cl^-S^{2-} - 238.717Na^+OH^- - 27.063O^{2-}P^{5+} \end{aligned} \quad (9)$$

where $Al^{3+}, Ca^{2+}, Cl^{-}, F^{-}, Fe^{2+}, K^{+}, Mg^{2+}, Na^{+}, O^{2-}, OH^{-}, P^{5+}, Si^{4+}$ and S^{2-} are the numbers of ions in molecule, of aluminum, calcium, chloride, fluoride, ferric, potassium, magnesium, sodium, oxygen, hydroxide, phosphorus, silicon, and sulfur, respectively.

Using these correlations, the average relative errors (REs) are 1.3, 1.0, and 1.4% for T_c, P_c, and T_b, respectively.

On the basis of the reactions taking place in industrial phosphoric acid[21,22] and on impurities content from laboratory analysis of concentrated phosphoric acid, the major impurities constituting the pseudocomponent with their characterization calculated by Eq. (10), are given in Table 2.

$$D_{PC} = \sum_i X_i D_i \tag{10}$$

where X_i is the average mass fraction of substance i in the pseudocomponent. D_i and D_{PC} are the ions number of the same type in molecule i and in the pseudocomponent, respectively.

To use PR EOS, the critical properties, T_c and P_c, and boiling temperature of the pseudocomponent were estimated by Eqs. (7)–(9), respectively, using its characterization data, given in the last row of Table 2 while the acentric factor of this pseudocomponent is calculated using Eq. (4).

Estimation of Phosphoric Acid Substance Properties

For phosphoric acid substance, many thermodynamic data are not available. Therefore, it was necessary to estimate physical properties from theoretically based correlations. Thus, estimates of critical temperature were based on modification of the Guldberg–Guye rule[29] using Eq. (11), while critical pressure and critical volume were based on the Herzog proposal[29] and the Benson relation,[29] respectively, using Eqs. (12) and (13).

The liquid density at boiling point temperature was calculated from Mathia relation[29] with Eq. (15).

The acentric factor was calculated using Eq. (4).

All these correlations are given below:

$$\frac{T_b}{T_c} = 0.614 \tag{11}$$

$$P_c = 21.75\frac{T_c}{v_c} \tag{12}$$

$$v_c = v_b(0.422\,\mathrm{Log}\,P_c + 1.981) \tag{13}$$

Table 2. Pseudocomponent Characterization Data

Substance	X_i	Al^{3+}	Ca^{2+}	Cl^-	F^-	Fe^{2+}	K^+	Mg^{2+}	Na^+	O^{2-}	OH^-	P^{5+}	S^{2-}	Si^{4+}
$Al(H_2PO_4)_3$	0.011	0.011	0	0	0	0	0	0	0	0.066	0.066	0.033	0	0
CaF_2	0.045	0	0.045	0	0.090	0	0	0	0	0	0	0	0	0
$Ca(H_2PO_4)_2$	0.11	0	0.110	0	0	0	0	0	0	0.440	0.440	0.220	0	0
$CaSiF_6$	0.086	0	0.086	0	0.516	0	0	0	0	0	0	0	0	0.086
$CaSO_4$	0.466	0	0.466	0	0	0	0	0	0	1.864	0	0	0.466	0
$Fe(H_2PO_4)_2$	0.048	0	0	0	0	0.048	0	0	0	0.192	0.192	0.096	0	0
K_2SiF_6	0.004	0	0	0	0.024	0	0.008	0	0	0	0	0	0	0.004
K_3AlF_6	0.009	0.009	0	0	0.054	0	0.027	0	0	0	0	0	0	0
$MgCl_2$	0.077	0	0	0.154	0	0	0	0.077	0	0	0	0	0	0
$MgSiF_6$	0.135	0	0	0	0.810	0	0	0.135	0	0	0	0	0	0.135
Na_2SiF_6	0.003	0	0	0	0.018	0	0	0	0.006	0	0	0	0	0.003
Na_3AlF_3	0.006	0.006	0	0	0.018	0	0	0	0.018	0	0	0	0	0
PC	1	0.026	0.707	0.154	1.530	0.048	0.035	0.212	0.024	2.562	0.698	0.349	0.466	0.228

$$v_b = \frac{M}{\varphi_b^L} \tag{14}$$

$$\rho_b^L = \rho^L \left(\frac{2T_c - T_b}{2T_c - 298} \right) \tag{15}$$

where ρ^L is the liquid density at 25°C.

The pure phosphoric acid boiling point temperature at 1.013 bar was estimated by the extrapolation of vapor pressure vs. temperature for phosphoric acid–water binary mixture.[30]

The thermodynamic properties for the phosphoric acid substance and the pseudocomponent are given in Table 3.

Estimation of Binary Interaction Parameters

Water–Phosphoric Acid Binary Interaction Parameter

The binary interaction parameter for water–phosphoric acid mixture was adjusted by Elyadari and Bouanani[31] using experimental vapor pressure data of this binary system.[30]

In this work, parameter estimation was performed using maximum likelihood principle[28] by comparing experimental and calculated saturation temperatures. The latter was computed from Eq. (5). The resulting optimization problem was solved by Davidon's method.[32]

Water–Pseudocomponent Pseudo-Binary Interaction Parameter

Due to the complexity of the industrial phosphoric acid impurity composition, and the difficulty in monitoring of this composition, it is not easy, for industrial purpose, to update the characterization data of the pseudocomponent.

Table 3. Phosphoric Acid Substance and Pseudocomponent Thermodynamic Properties with Results of Binary Interaction Parameter Estimation

	T_b (K)	T_c (K)	P_c (bar)	ω	δ_{ij}	MARE (%)
H_3PO_4	505	822.5	103.78	0.3703		
Pseudocomponent	690	1100	50.66	0.2213		
Phosphoric acid–water					−0.17	0.71
Pseudocomponent–water					−0.42	0.25

Hence, for practical use of the approach proposed in the present work, we assumed that data characterization are constant.

To compensate for this approximation, the pseudo-binary interaction parameter between water and the pseudocomponent should be estimated using VLE data of the industrial phosphoric acid. This procedure is a substitute to detailed composition data of industrial phosphoric acid impurities, the VLE data of this acid being easier to obtain.

A similar procedure was used successfully for VLE modeling of industrial cane and beet sugar juices.[23]

For doing this, in the present work the binary interaction parameter for water–phosphoric acid and flash data from a boiler of a phosphoric acid concentration process, were used to identify the pseudo-binary interaction parameter between water and the pseudocomponent. Indeed, the average bubble pressure and the average composition of phosphoric acid for a cycle were used to calculate the boiling temperature. Several process cycles were used for this estimation (Table 4). The boiling temperature was calculated for industrial phosphoric acid by means of Eq. (5) and was compared to the average boiling temperature for each cycle of the same concentration process.

To estimate this interaction pseudo-binary parameter, Fibonacci optimization method[33] was used to minimize the following objective function:

$$\mathrm{OF} = \sum_{i=1}^{\mathrm{NC}} \left(\bar{T}^{i}_{\mathrm{prdata}} - T^{i}_{\mathrm{cal}} \right)^2 \tag{16}$$

where NC is number of cycles. The subscripts prdata and cal refer to process data and calculated temperature corresponding to cycle i.

Table 4. VLE Data for Industrial Phosphoric Acid

Cycle Number	$x_{H_3PO_4}$	x_{imp}	$\bar{T}^{boil}$ (K)	$\bar{P}^{boil}$ (bar)
1	0.739	0.061	350.15	0.089
2	0.740	0.053	349.85	0.094
3	0.731	0.085	351.85	0.082
4	0.730	0.080	350.44	0.083
5	0.730	0.075	350.15	0.085
6	0.720	0.078	349.65	0.084
7	0.720	0.090	350.85	0.083
8	0.730	0.077	350.35	0.085
9	0.734	0.074	349.55	0.081
10	0.726	0.085	350.65	0.083
11	0.732	0.078	349.65	0.080

The binary interaction parameter between phosphoric acid and the pseudocomponent was missed.

The values of binary interaction parameters δ_{ij} with the mean absolute relative error (MARE) on boiling point are presented in Table 3. As can be seen, this value of pseudo-binary interaction parameter of water-pseudocomponent is very high. This is due to the assumption described in the section explaining parameter estimation.

Estimation of Vapor Pressure

Because the PR EOS gives a poor estimation for the phosphoric acid and water vapor pressures, this property was calculated using Eq. (17).

$$\mathrm{Ln}\, P_i^{\mathrm{V}} = A_i + \frac{B_i}{T + C_i} + D_i T^2 + E_i T^6 + F_i \,\mathrm{Ln}\, T \tag{17}$$

where A_i, B_i, C_i, D_i, E_i, and F_i are the correlation coefficients corresponding to pure substance i.

For phosphoric acid substance, the expression coefficients were fitted using experimental vapor pressure data for water–phosphoric acid binary mixture[30] by multiple stepwise regression technique.[28]

While for the pseudocomponent, the Riedel's equation for vapor pressure[33] was used to estimate expression coefficients of the vapor pressure. The constants for Riedel's correlation are calculated from critical properties and boiling point temperature of pseudocomponent.

Table 5 represents the coefficients of vapor pressure expression of Eq. (17) for phosphoric acid and pseudocomponent.

Estimation of Ideal Gas Heat Capacity

The ideal gas heat capacity of water, phosphoric acid substance, and pseudocomponent was presented as following functional form:

$$Cp_i^0 = a_i + b_i T + c_i T^2 + d_i T^3 + \frac{e_i}{T} \tag{18}$$

where a_i, b_i, c_i, d_i, and e_i are constants corresponding to pure component i.

Table 5. Phosphoric Acid Substance and Pseudocomponent Vapor Pressure Expression Coefficients

	A_i	B_i	C_i	D_i	E_i	F_i
H_3PO_4	7.8662	−6641.5143	0.00	0.00	0.00	0.00
Pseudocomponent	39.4448	−10692.00	0.00	0.00	5.64×10^{-19}	−4.384

The ideal gas heat capacity for phosphoric acid component was predicted by the method of Harrison and Seaton.[34] The calculated values of ideal gas heat capacity over temperature range from 300–1500K, were used to fit coefficients of Eq. (18) using multiple stepwise regression.

For the pseudocomponent, the ideal gas heat capacity coefficients were determined using a group contribution technique. The ideal gas heat capacity coefficients data[26] for the 27 pure compounds model of Table 1 were used to develop correlations relating a_i, b_i, c_i, d_i, and e_i coefficients to ionic characterization data, using multiple stepwise regression.

The correlations obtained are the following:

$$\begin{aligned} a_{PC} = {} & 19.801 - 24.898Al^{3+} - 23.957(Ca^{2+})^2 + 13.182Cl^- \\ & + 18.023F^- - 5.353K^+ + 4.884(Mg^{2+})^{-1} - 5.679Na^+ \\ & + 4.606O^{2-} + 7.266OH^- + 11.083P^{5+} + 2.601S^{2-} \\ & + 4.285Cl^-Fe^{2+} + 6.772Cl^-(OH^-)^{1/2} - 14.440Cl^-P^{5+} \\ & + 0.080(Cl^-)^2Si^{4+} - 0.354(Cl^-)^2O^{2-} - 4.916O^{2-}P^{5+} \\ & - 18.179O^{2-}(S^{2-})^2 \end{aligned} \tag{19}$$

$$\begin{aligned} b_{PC} = {} & -0.007 + 0.152Al^{3+} + 0.162(Ca^{2+})^{-2} + 0.019Cl^- \\ & - 0.031F^- - 0.021Fe^{2+} + 0.046K^+ - 0.021Mg^{2+} \\ & + 0.039Na^+ + 0.086O^{2-} - 0.038(O^{2-})^{-1} + 0.110OH^- \\ & + 0.095P^{5+} + 0.081(S^{2-})^{1/2} - 0.099(Si^{4+})^{-1} \\ & + 0.012(Cl^-)^2P^{5+} + 0.078Cl^-(Si^{4+})^{-1} \\ & - 0.078(OH^-)^{1/2}S^{2-} \end{aligned} \tag{20}$$

$$\begin{aligned} c_{PC} = {} & 10^{-6}(58 - 308Al^{3+} - 24Cl^- + 75F^- - 7.12Fe^{2+} - 137K^+ \\ & - 11Mg^{2+} - 121Na^+ - 171O^{2-} + 113(O^{2-})^{-1} - 177OH^- \\ & - 74P^{5+} - 132(S^{2-})^{1/2} + 206(Si^{4+})^{-1} - 163(Ca^{2+})^{-2}F^- \\ & - 79Cl^-P^{5+} - 9.956(Cl^-)^2P^{5+} - 164Cl^-(Si^{4+})^{-1} \\ & + 232(OH^-)^{1/2}S^{2-}) \end{aligned} \tag{21}$$

$$d_{PC} = 10^{-7}(2.261Al^{3+} + 2.130Ca^{2+} - 0.740F^{-} + 0.021Fe^{2+} + 0.770K^{+} - 0.073Mg^{2+} + 0.645Na^{+} + 1.322O^{2-} - 1.147(O^{2-})^{-1} + 1.137OH^{-} + 1.616(P^{5+})^{-1} + 0.768(S^{2-})^{1/2} - 2.045(Si^{4+})^{-1} + 1.516Cl^{-}(Si^{4+})^{-1} + 0.159(Cl^{-})^{2}P^{5+} - 2.056S^{2-}(OH^{-})^{1/2}) \quad (22)$$

$$e_{PC} = 10^{-11}(0.935 - 5.887Al^{3+} - 5.509Ca^{2+} - 0.261Cl^{-} + 1.649F^{-} - 0.296Fe^{2+} - 2.676K^{+} - 0.428Mg^{2+} - 2.360Na^{+} - 3.713O^{2-} + 3.202(O^{2-})^{-1} - 3.322OH^{-} + 3.591(P^{5+})^{-1} - 1.781(S^{2-})^{1/2} + 4.866(Si^{4+})^{-1} - 3.512Cl^{-}(Si^{4+})^{-1} - 4.289Cl^{-}P^{5+} + 0.152(Cl^{-})^{2}P^{5+} + 5.929(OH^{-1})^{1/2}S^{2-}) \quad (23)$$

The average REs for the coefficients regressions a_{PC}, b_{PC}, c_{PC}, d_{PC}, and e_{PC} are 1.3, 2.7, 2.5, 2.4, and 2.0%, respectively.

Equations (19)–(23) were used to calculate ideal gas heat capacity coefficients for pseudocomponent using its ionic characterization data presented in the last row of Table 2.

The coefficients corresponding to phosphoric acid substance and to pseudocomponent are represented in Table 6.

For water, critical data, boiling point, vapor pressure coefficients, and ideal gas heat capacity coefficients were taken from the literature.[26]

Prediction of Heat Capacity of Precipitated Mineral Salts

As has been mentioned, the industrial phosphoric acid usually contains a quantity of solid materials. The latter, of course did not present in VLE calculations, but it contributed to the calculation of the mixture enthalpy.

Heat capacity of this precipitated solid was determined by Mostafa's method[35] based on group contribution technique.

Table 6. Ideal Gas Heat Capacity Coefficients of Phosphoric Acid Substance and Pseudocomponent

C_p^0	a_i	b_i	c_i	d_i	e_i
H_3PO_4	84.37	9.83×10^{-2}	-33×10^{-6}	0.00	−7631.253
Pseudocomponent	50.42	32.4×10^{-2}	-356×10^{-6}	4.55×10^{-7}	1187.13

By application of this technique for the pseudocomponent and using characterization data given in the last row of Table 2, its heat capacity expression at solid state was given by relation (24).

$$C_{p\,\mathrm{PC}}^{\mathrm{solid}} = 302.691 - 0.368T + 622 \times 10^{-6}T^2 - 3.415 \times 10^{-7}T^3 - \frac{29940.99}{T} \tag{24}$$

The enthalpy of vapor and liquid phases was calculated using PR EOS. Because of the low value of the boiler pressure, the vapor phase can be considered as ideal.

For the industrial phosphoric acid mixture enthalpy calculation, we must add the enthalpy of the solid salts to that of the liquid phase.

SCAPE SIMULATION SYSTEM

Because of their complexity, the tasks of process design and analysis are increasingly conducted with the aid of computers, and many simulation packages for chemical and petrochemical process have been developed (ASPEN-Plus, PRO II, High Sim, etc.). The latter were used especially for the hydrocarbons. Therefore, an objective of the research being conducted in our laboratory for several years was to develop a process simulator named SCAPE for the food and ore-processing industries. The SCAPE software (software for computer aided process engineering) was developed following the same modular sequential approach, used by many other simulation packages. It is a steady-state simulator.

The system is continually being improved and expanded by new unit operations modules, new physical properties routines, new compounds added to the data bank, which include three types of substances: fluid, ionic, and solid mineral substances.

The SCAPE software contains three important blocks:

- PHYSCAPE software can be used to generate the physical properties for pure components and mixtures using the thermodynamic models and

estimating techniques or fitting experimental data. It also allows to determinate VLE calculations.

- VALISCAPE is a data reconciliation software. It uses information redundancy and conservation laws to reconcile the measurements. VALISCAPE detects faulty sensors and pinpoints degradation of equipment performance (heat rate, compressor efficiency, etc.). Data reconciliation exploits information redundancy and conservation laws to extract accurate and reliable information from measurements.
- SIMSCAPE software can be used for steady-state simulation of industrial processes. In this software, the model equations are handled using the library of modules, each of which perform computations for one of the models used.

STEADY-STATE SIMULATION OF PHOSPHORIC ACID MIXTURE CONCENTRATION PROCESS

The simulation sequence calculation of the process under study is shown in Fig. 2. The SIMSCAPE library modules used are: HEX010, MIX010, FLH010, DIV010, which were used for modeling heat exchanger, mixer, boiler and pumps, and splitter, respectively. The MAT020 module is used for convergence promotion on the tear stream.

In order to start the calculations, the temperature, pressure, and flow rate values for the recycled stream have been guessed based on the process data. The modules were then called in the sequence shown in Fig. 2, until new values for the tear stream were generated. The heat and material balances equations system was then solved iteratively by Rubin convergence algorithm. It was used to converge within a preset tolerance of about 10^{-6}.

Because the flow-sheet equations solving method requires a reasonably good initial guess, there has been severe problem to converge the calculations. To improve the convergence, sometimes temperature and mass flow rate initializations of the recycled stream must be changed.

The fundamental equation for heat transfer rate in the heat exchanger is:

$$Q = UA_{\text{eff}}F\,\text{LMTD} \tag{25}$$

where Q is the exchanged heat rate, U the overall heat transfer coefficient, A_{eff} the effective heat transfer area, F heat exchanger efficiency, and LMTD the log mean temperature difference.

The lumped parameter $UA_{\text{eff}}F$ coefficient was used in this work to characterize the heat exchanger scaling.

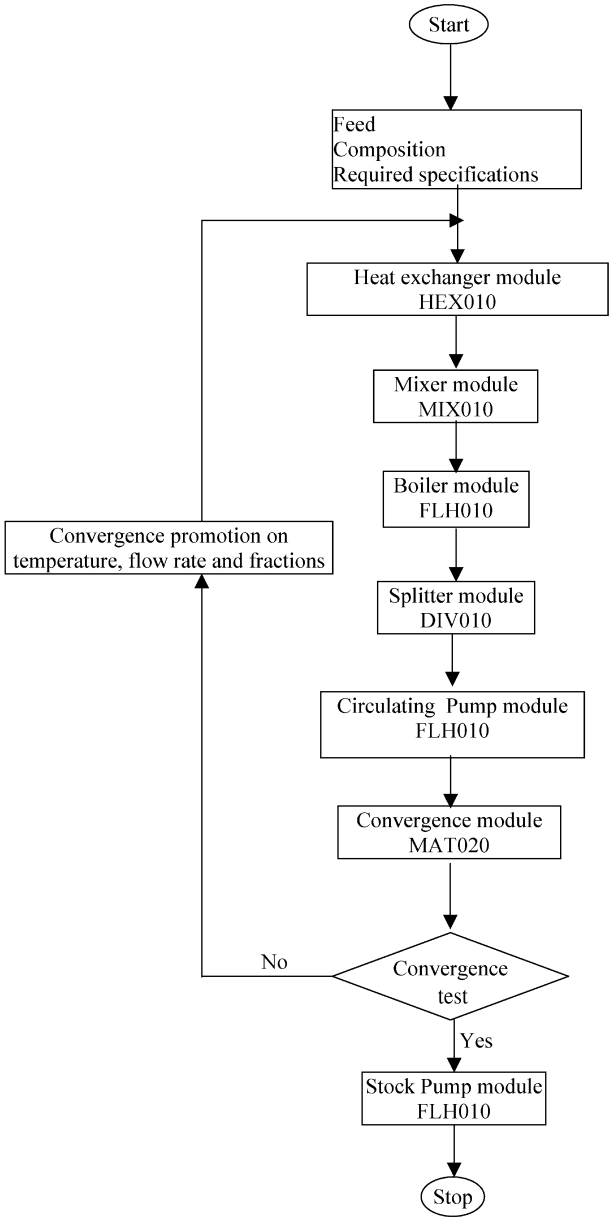

Figure 2. Flow chart for concentration process rating calculations.

Simulation Results and Discussion

The modular sequential steady-state simulations of concentration process (Fig. 2) over a cycle of 176 hr were successfully carried out. These reproduced plant operations satisfactorily. Feed and operating conditions were dependent on the time and were listed in Table 7, but since the pseudo-steady-state was assumed, the time was not taken into account in the simulation. The splitter ratio was chosen in such a way that recycled phosphoric acid mass flow rate was constant, during all cycle time ($fl^{rec} = 3795\,t/hr$). The stock pump pressure was equal to 6.91 bar. As for weak acid feed, the mass composition of impurities was set to 3.8% and that of solid to 1%.

Process data and simulation results are given in Table 7. The RE corresponding to the calculated values of boiler and heat exchanger outlet temperatures, and concentrated phosphoric acid flow rate are also given in this table. As can be seen from the table, a good agreement between process data and the simulation results is obtained. The MARE corresponding to heat exchanger temperature outlet, boiler temperature, P_2O_5 mass content, and mass flow rate of concentrated acid, are about 0.9, 0.4, 0.3, and 0.4%, respectively.

It should be noted from Table 7 and Figs. 3 and 4 that boiler temperature, P_2O_5 mass content, and $UA_{eff}F$ parameter value, which characterize the heat

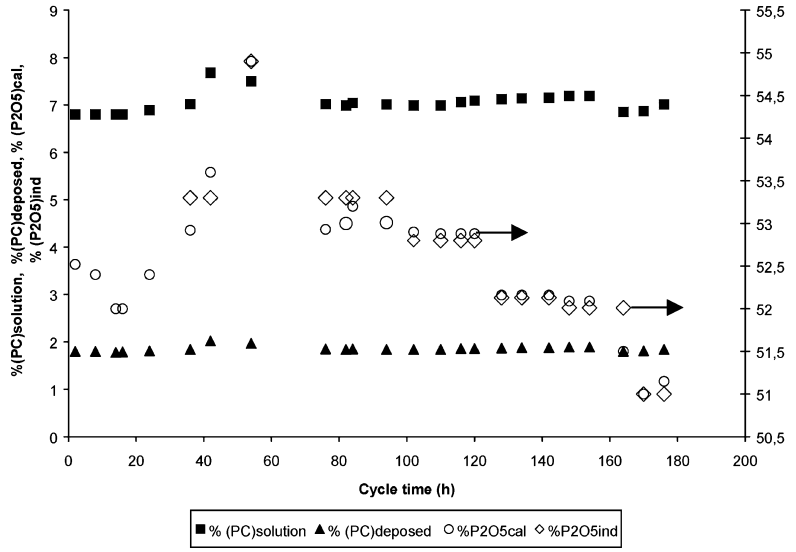

Figure 3. Calculated mass contents of pseudocomponent, comparison between calculated and industrial P_2O_5 mass content of concentrated phosphoric acid vs. cycle time.

Table 7. Process Data and Simulation Results

Cycle Time (hr)	fl^{wa} (t/hr)	$(P_2O_5)^{wa}$ (%)	fl^{steam}_{prdata} (t/hr)	P^{steam} (bar)	P^{boil} (bar)	P^{circ} (bar)	T^{boil}_{prdata} (K)	Relative Error (%)	$T^{outexch}_{ind}$ (K)	Relative Error (%)	fl^{conc}_{prdata} (t/hr)	Relative Error (%)
2	79.09	30.00	42.12	3.213	0.083	4.46	350.15	−0.19	362.15	0.14	43.99	−0.66
8	79.63	29.85	42.12	3.213	0.080	4.46	348.15	−0.44	360.15	0.01	44.39	−0.24
14	76.03	29.85	40.03	3.613	0.085	4.35	349.15	−0.18	363.15	−2.91	42.77	−0.68
16	76.03	29.85	40.00	3.513	0.085	4.39	349.15	−0.06	362.15	−1.75	42.77	−0.68
24	74.77	29.85	40.00	3.513	0.082	4.42	349.15	0.32	362.15	−1.23	41.26	−0.17
36	73.08	29.85	40.00	3.013	0.079	4.89	350.15	−0.06	360.15	1.86	39.49	0.00
42	60.12	28.69	36.00	3.013	0.068	5.41	350.15	0.83	362.15	−0.51	29.52	0.60
54	62.14	30.00	36.00	2.813	0.060	4.28	349.15	0.49	361.15	−0.59	31.32	0.34
76	73.08	29.85	40.00	3.913	0.076	4.90	348.15	1.47	361.15	−0.13	39.49	0.09
82	72.36	30.00	40.00	4.013	0.080	4.53	350.15	0.26	361.15	0.90	39.71	−1.01
84	72.72	30.00	40.00	4.013	0.080	4.42	351.15	−0.32	362.15	0.60	39.71	0.27
94	72.07	30.00	40.00	4.113	0.083	4.59	351.15	0.19	363.15	−0.28	39.49	−1.10
102	72.65	30.00	40.00	4.113	0.080	4.47	351.15	−0.02	363.15	−0.42	39.60	−0.36
110	72.36	30.00	40.00	3.313	0.080	4.36	351.15	−0.97	361.15	0.84	39.35	−0.09
116	72.68	29.78	40.00	3.513	0.080	4.61	351.15	−0.79	361.15	1.29	39.35	−0.64
120	71.35	29.64	40.00	3.513	0.082	4.43	351.15	−0.71	361.15	1.18	38.05	0.28
128	64.58	28.97	36.00	3.513	0.086	4.77	350.15	0.71	361.15	−0.01	34.45	−0.10
134	62.21	28.91	34.99	3.413	0.085	4.70	350.15	0.45	361.15	−0.57	33.08	−0.11
142	62.42	28.62	34.99	3.413	0.088	4.83	350.15	0.57	361.15	−0.57	33.08	0.11
148	61.97	28.62	34.99	3.613	0.084	5.08	350.15	−0.06	361.15	−1.09	32.90	−0.66
154	61.97	28.62	34.99	3.613	0.084	5.08	350.15	−0.06	361.15	−1.09	32.80	−0.33
164	70.74	29.34	37.98	3.713	0.088	5.31	349.15	−0.06	358.15	1.90	39.35	−0.27
170	76.97	28.98	42.12	4.213	0.090	5.31	348.15	0.86	361.15	−0.73	42.52	0.08
176	75.42	28.54	42.12	4.013	0.084	5.30	348.15	−0.33	359.15	0.54	40.86	0.00

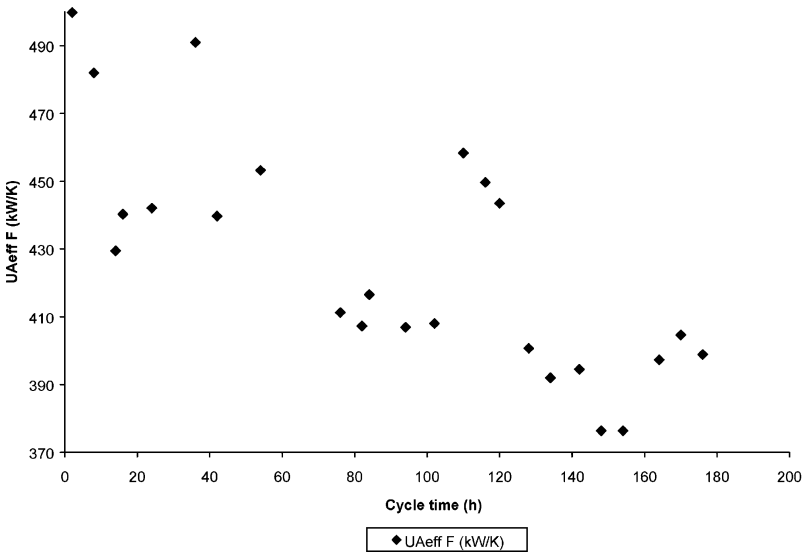

Figure 4. $UA_{\text{eff}}F$ coefficient vs. cycle time.

exchanger scaling, decreased after about 120 hr of cycle time. Indeed, during concentration, the solubility of many salts present in phosphoric acid solution was exceeded, and precipitation and deposition of solid on the heat exchanger surfaces occurred. According to this work, this caused about a 3K drop in boiler temperature, about a 2% drop in P_2O_5 mass content of concentrated phosphoric acid, and a 70 kW/K drop in $UA_{\text{eff}}F$ parameter value because the overall heat transfer coefficient also decreased. The P_2O_5 mass content of weak phosphoric acid also decreased after about 130 hr; this can also involve the decrease in P_2O_5 mass content of concentrated acid.

When the scale was deposited on the heat exchanger surfaces, the $UA_{\text{eff}}F$ parameter value decreased, so the exchanged heat also decreased. Hence, P_2O_5 mass content of concentrated phosphoric acid and therefore boiling temperature decreased.

As can be seen in Fig. 4, the $UA_{\text{eff}}F$ parameter value increased for the last three cycle points with the steam mass flow rate, in order to improve the concentration quality. Indeed, the condensate circulation was improved by the increase in steam flow rate in the heat exchanger, which appeared in the rise of the heat transfer coefficient value.

According to this study, it appeared that the model used to simulate phosphoric acid concentration process can be suitable to study the sensitivity vs. the process important variables.

Sensitivity Analysis

Sensitivity analysis was performed to study the effect of the main process variables on the process behavior. The variables tested are: steam and weak phosphoric acid mass flow rates, boiler pressure and mass content of impurities in the weak phosphoric acid.

Figures 5–8 give sensitivity analysis results corresponding to these variables. The interpretation of all the trends obtained is evident.

Indeed, with increase in steam flow rate, much water is evaporated in the boiler (Fig. 5), but for the same amount of the heat exchanged, the acid produced will be less concentrated if the weak acid flow rate increased (Fig. 6). The same trend is observed if the boiler temperature increased by the effect of the increase in the boiler pressure (Fig. 7) or the impurities mass content of feed acid (Fig. 8).

CONCLUSIONS

In the present work, an attempt to adapt the PR EOS for industrial phosphoric acid using the pseudocomponent approach was made. Industrial phosphoric acid was constituted by two phases, liquid phase considered as

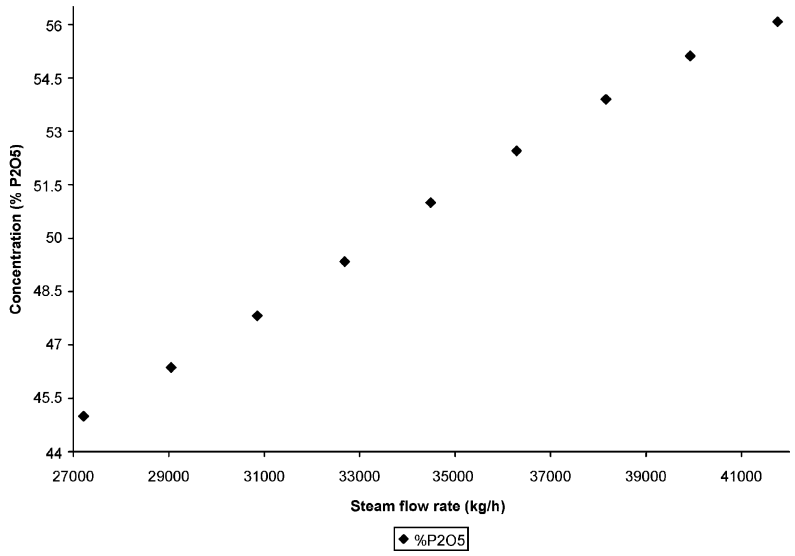

Figure 5. Sensitivity of P_2O_5 mass content of concentrated phosphoric acid toward steam mass flow rate.

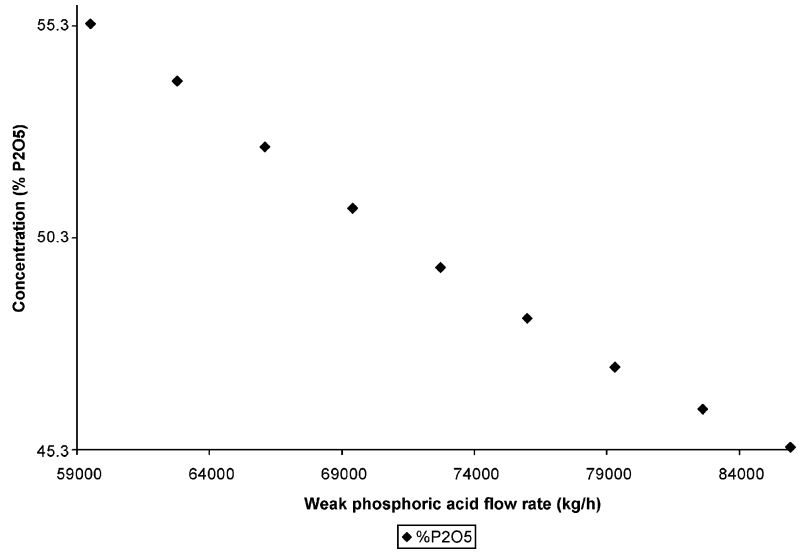

Figure 6. Sensitivity of P_2O_5 mass content of concentrated phosphoric acid toward weak phosphoric acid mass flow rate.

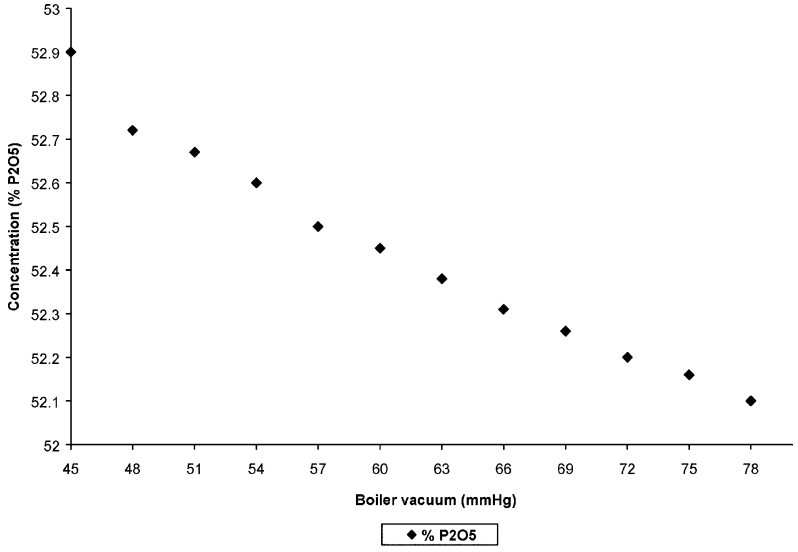

Figure 7. Sensitivity of P_2O_5 mass content of concentrated phosphoric acid toward boiler pressure.

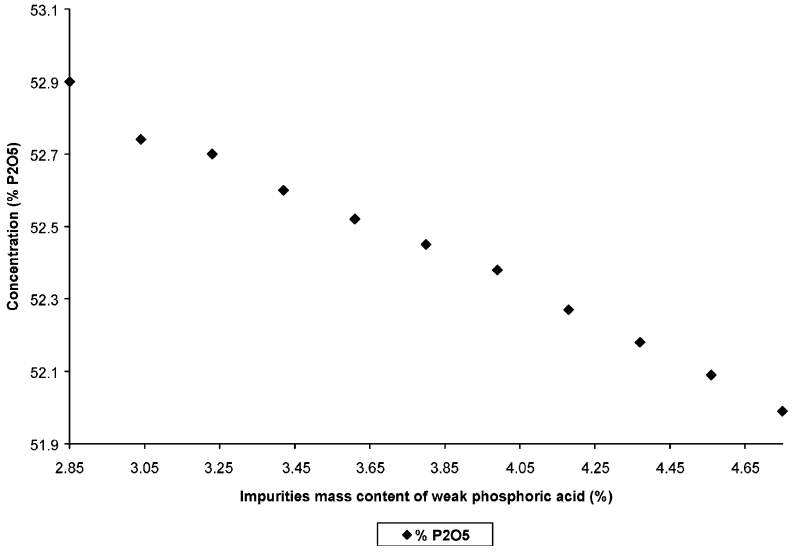

Figure 8. Sensitivity of P_2O_5 mass content of concentrated phosphoric acid toward impurities mass content of weak phosphoric acid feed.

ternary system of phosphoric acid, water, and impurities. The latter were represented by pseudocomponent and solid phase, which was characterized by the same pseudocomponent. The composition of the latter could be obtained from composition of industrial phosphoric acid.

The SCAPE simulator developed previously in our laboratory was used for process simulation. The results obtained agree well with the real plant data.

Sensitivity analysis was performed for the main process variables: steam and weak acid flow rates, P_2O_5 and impurities content of the feed acid and the boiler pressure. The trends obtained correspond to the normal behavior of the real plant.

NOMENCLATURE

A	heat exchanger area (m^2)
C_p	heat capacity (kJ/kmol K)
D	number of ions
F	heat exchanger efficiency
M	molar mass (kg/mol)
N	number of components in mixture

NC	number of cycles
OF	objective function
P	absolute pressure (bar)
$\bar{P}$	mean pressure of cycle (bar)
Q	thermal exchanged heat (kW)
R	universal gas constant (kJ/mol/K)
T	temperature (K)
$\bar{T}$	mean temperature of cycle (K)
U	overall heat transfer coefficient (kW/m^2/K)
X	average mass fraction
a	PR EOS constant [atm (m^3/mol)^2]
b	PR EOS constant (m^3/mol)
f	fugacity
fl	total mass flow rate (t/hr)
v	molar volume (m^3/kmol)
Z	mixture mole fraction
Al^{3+}	number of aluminum ions
Ca^{2+}	number of calcium ions
Cl^-	number of chloride ions
F^-	number of fluoride ions
Fe^{2+}	number of ferric ions
K^+	number of potassium ions
Mg^{2+}	number of magnesium ions
Na^+	number of sodium ions
O^{2-}	number of oxygen ions
OH^-	number of hydroxide ions
P^{5+}	number of phosphorus ions
S^{2-}	number of sulfur ions
Si^{4+}	number of silicon ions

Greek letters

δ	binary interaction parameter
ϕ	fugacity coefficient
ρ	density (kg/m^3)
ω	acentric factor

Subscripts

b	boiling (K)
c	critical (K)
cal	calculated
eff	effective
i	component i

imp	Impurities
prdata	process data
j	component *j*
k	component *k*
m	mixture
PC	pseudocomponent

Superscripts

boil	boiler
circ	circulating
conc	concentrated
L	liquid
outexch	outlet of exchanger
rec	recycled
V	vapor
wa	weak acid
0	relative to ideal gas

Abbreviations

EOS	equation of state
LMTD	log mean temperature difference (K)
MARE	mean absolute relative error
PR	Peng–Robinson
RE	relative error
VLE	vapor–liquid equilibrium

REFERENCES

1. Pandey, A.D.; Mallick, K.K.; Pandey, P.C.; Varma, S. Prevention of Scale Deposition on Heat Exchanger Surfaces by Use of High Intensity Ultrasonic Waves During Concentration of Wet Process Phosphoric Acid. Fert. News **1983**, *June*, 45–48.
2. Sanatgar, H.; Somerscales, E.F.C. Account for Fouling in Heat Exchanger Design. Chem. Eng. Prog. **1991**, *December*, 53–59.
3. Georgiadis, M.C.; Rotstein, G.E.; Macchietto, S. Modeling and Simulation of Shell and Tube Heat Exchangers Under Milk Fouling. AIChE J. **1998**, *44*, 959–970.
4. Frenier, W.W.; Barber, S.J. Choose the Best Heat Exchanger Cleaning Method. Chem. Eng. Prog. **1998**, *July*, 37–44.

5. Wakefield, Z.T.; Luff, B.B.; Reed, R.B. Heat Capacity and Enthalpy of Phosphoric Acid. J. Chem. Eng. Data **1972**, *17*, 420–423.
6. Luff, B.B. Heat Capacity and Enthalpy of Phosphoric Acid. J. Chem. Eng. Data **1981**, *26*, 70–74.
7. Jiang, C. Thermodynamics of Aqueous Phosphoric Acid Solution at 25°C. J. Chem. Eng. Sci. **1996**, *51*, 689–693.
8. Nriagu, J.O. Lead Orthophosphates. I. Solubility and Hydrolysis of Secondary Lead Orthophosphate. Inorg. Chem. **1972**, *11*, 2499–2503.
9. Platford, R.F. Thermodynamics of the System H_2O–NaH_2PO_4–H_3PO_4. J. Chem. Eng. Data **1976**, *21*, 468–469.
10. Surdo, A.L.; Bernstrom, K.; Jonsson; Millero, F.J. Molal Volume and Adiabatic Compressibility of Aqueous Phosphate Solutions at 25°C. J. Phys. Chem. **1979**, *83*, 1255–1262.
11. Sullivan, J.M.; Kohler, J.J.; Grinstead, J.H., Jr. Effect of Aluminum, Iron, and Magnesium upon the Solubility of α-Calcium Sulfate Hemihydrate in 40%, 45%, 50%, and 55% P_2O_5 Phosphoric Acid Solutions at 80, 90, 100, and 110°C: Correlations with Water Concentration. J. Chem. Eng. Data **1991**, *36*, 77–80.
12. Achard, C.; Dussap, C.-G.; Gros, J.-B. Prediction of pH in Complex Aqueous Mixtures Using a Group-Contribution Method. AIChE J. **1994**, *40*, 1210–1222.
13. Cate, W.E.; Deming, M.E. Effect of Impurities on Density and Viscosity of Simulated Wet-Process Phosphoric Acid. J. Chem. Eng. Data **1970**, *15*, 290–295.
14. Mathias, P.M.; Mendez, M. Simulation of Phosphoric Acid Production by the Dihydrate Process. 22nd Clearwater Convention on Phosphate Fertilizer and Sulfuric Acid Technology. ASPEN Technology, Inc., May 22–23, 1998.
15. Yeo, Y.K.; Cho, Y.S.; Park, W.H.; Moon, B.K. Simulation of the Dihydrate Process for the Production of Phosphoric Acid. Korean J. Chem. Eng. **1991**, *8*, 23–32.
16. Giola, F.; Mura, G.; Viola, A. Analysis Simulation, and Optimization of the Hemihydrate Process for the Production of Phosphoric Acid from Calcareous Phosphorites. Ind. Eng. Chem., Process Des. Dev. **1977**, *16*, 390–399.
17. Cho, H.J.; Yeo, Y.K.; Park, W.H.; Moon, B.K. Modeling and Simulation of a Wet Hemihydrate Phosphoric Acid Process. Korean J. Chem. Eng. **1996**, *13*, 585–595.
18. Shakourzadeh, K.; Bloise, R.; Baratin, F. Modeling of Wet-Process Phosphoric Acid Reactor: Influence of Phosphate Rock Impurities. Proc.-Int. Congr. Phosphorus Compd. 2nd, 1980; 443–454.

19. Halawa, J.; Zielinski, S. Computer Simulation of Gypsum Crystallization in Wet Phosphoric Acid Processes. Ind. Cryst., Proc. Symp. 8th, 1982; 345–346.
20. Steemson, M.L.; Mukhopadhyay, S.; White, E.T. Gypsum Crystallization in Wet Phosphoric Acid Manufacture: Options for Process Improvement. Chemeca 85: Innovation Process Resour. Ind., Aust. Chem. Eng. Conf. 13th, 1985; 225–230.
21. Slack, A.V. Concentration of Wet Process Acid. *Phosphoric Acid*; Marcel Dekker, Inc.: New York, 1968; Vol. 1, 579–634.
22. Becker, P. Acid Concentration Systems, Product Acid Impurities and Sludge. *Phosphates and Phosphoric Acid*; Marcel Dekker, Inc.: New York, 1983; 405–440.
23. Abderafi, S.; Bounahmidi, T. Measurement and Estimation of Vapor–Liquid Equilibrium for Industrial Sugar Juice Using the Peng–Robinson Equation of State. Fluid Phase Equilibria **1999**, *162*, 225–240.
24. Alexander, G.L.; Schwartz, B.J.; Prausnitz, J.M. Phase Equilibria for High-Boiling Fossil-Fuel Distillates. 2. Correlation of Equation of State Constants with Characterization Data for Phase-Equilibrium Calculations. Ind. Eng. Chem. Fund. **1985**, *24*, 311–315.
25. Peng, D.Y.; Robinson, D.B. A New Tow-Constant Equation of State. J. Ind. Eng. Chem. Fund. **1976**, *15*, 59–64.
26. Yaws, C.L. Critical Properties and Acentric Factor, Heat Capacity of Gas. *Chemical Properties Handbook*; McGraw-Hill: New York, 1999; 1–55.
27. Reid, R.C.; Prausnitz, J.M.; Poling, B.E. Thermodynamic Properties. *The Properties of Gases and Liquids*; McGraw-Hill: New York, 1987; 144–145.
28. Himmelblau, D.M. Linear Models with Several Independent Variables. *Process Analysis by Statistical Methods*; John Wiley & Sons, Inc.: New York, 1970; 143–175.
29. Perry Robert, H.; Chilton Cecil, H. *Chemical Engineers' Handbook*; 1973.
30. Othmer, K. *Encyclopedia of Chemical Technology*, 2nd Ed.; Interscience Publishers: New York, 1968; Vol. 15, 236.
31. Elyadari, A.; Bouanani, B. Analyse Assistée par Ordinateur du Procédé de Concentration d'Acide Phosphorique. Projet de Fin d'Etude, Ecole Mohammadia d'Ingénieurs.
32. Edgard, T.F.; Himmelblau, D.M. Unconstrained Multivariable Optimization. *Optimisation of Chemical Processes*; McGraw-Hill: New York, 1989; 220–224.
33. Raman, R. Estimation of Gas and Liquid Properties. *Chemical Process Computations*; Elsevier Applied Science Publishers Inc.: London and New York, 1985; 46–47.

34. Harrison, K.B.; Seaton, W.H. Solution to Missing Group Problem for Estimation of Ideal Gas Heat Capacities. Ind. Eng. Chem. Res. **1988**, *27*, 1536–1540.
35. Mostafa, G.A.T.M.; Eakman, J.M.; Montoya, M.M.; Yarbro, S.L. Prediction of Heat Capacities of Solid Inorganic Salts from Group Contributions. Ind. Eng. Chem. Res. **1996**, *35*, 343–348.

Received July 2001
Revised January 2002